TISSUE ENGINEERING: Part A
Volume 15, Number 7, 2009

DOI: 10.1089/ten.tea.2008.0364

Neural Stem Cell– and Schwann Cell–Loaded Biodegradable Polymer Scaffolds Support Axonal Regeneration in the Transected Spinal Cord

Heather E. Olson, M.D., Gemma E. Rooney, Ph.D., LouAnn Gross, Jarred J. Nesbitt, B.S., Katherine E. Galvin, Ph.D., Andrew Knight, Ph.D., BingKun Chen, M.D., Ph.D., Michael J. Yaszemski, M.D., Ph.D., and Anthony J. Windebank, M.D.

Biodegradable polymer scaffolds provide an excellent approach to quantifying critical factors necessary for restoration of function after a transection spinal cord injury. Neural stem cells (NSCs) and Schwann cells (SCs) support axonal regeneration. This study examines the compatibility of NSCs and SCs with the poly-lactic-co-glycolic acid polymer scaffold and quantitatively assesses their potential to promote regeneration after a spinal cord transection injury in rats. NSCs were cultured as neurospheres and characterized by immunostaining for nestin (NSCs), glial fibrillary acidic protein (GFAP) (astrocytes), βIII-tubulin (immature neurons), oligodendrocyte-4 (immature oligodendrocytes), and myelin oligodendrocyte (mature oligodendrocytes), while SCs were characterized by immunostaining for S-100. Rats with transection injuries received scaffold implants containing NSCs ($n = 17$), SCs ($n = 17$), and no cells (control) ($n = 8$). The degree of axonal regeneration was determined by counting neurofilament-stained axons through the scaffold channels 1 month after transplantation. Serial sectioning through the scaffold channels in NSC- and SC-treated groups revealed the presence of nestin, neurofilament, S-100, and βIII tubulin–positive cells. GFAP-positive cells were only seen at the spinal cord–scaffold border. There were significantly more axons in the NSC- and SC- treated groups compared to the control group. In conclusion, biodegradable scaffolds with aligned columns seeded with NSCs or SCs facilitate regeneration across the transected spinal cord. Further, these multichannel biodegradable polymer scaffolds effectively serve as platforms for quantitative analysis of axonal regeneration.

Introduction

The field of spinal cord repair and regeneration is rapidly advancing, primarily through translational research in animal models. After traumatic spinal cord injury (SCI), areas of gliotic scar tissue and areas of cystic degeneration create a structural barrier to regeneration and consequently return of function. Forty percent of patients with SCI have complete loss of function below the level of injury and no functioning neural tissue at the level of the injury.[1,2] Proposed methods for bypassing this damaged area of spinal cord include robotic or electronic connections or replacing the scar and cystic areas with either a nervous tissue bridge or a synthetic bridge.[3,4]

Biodegradable polymer scaffolds serve to form a structural support to bridge the injury site and guide axonal regeneration. An 85:15 polylactic acid:polyglycolic acid (PLGA) scaffold maintains its structural integrity for at least 8 weeks and starts to degrade significantly by 24 weeks.[5] Polylactic acid and polyglycolic acid polymers and their copolymers have been used extensively in clinical practice and have been found to be biocompatible.[6–8] Two clinical studies used PLGA guidance channels for peripheral nerve regeneration without significant adverse effects.[9,10] α-Hydroxy acid polymer scaffolds have been used extensively in animal models of peripheral nerve injury[11–13] and SCI.[14–16] The biodegradability of the scaffolds prevents long-term foreign body reaction, local damage, or need for further surgeries. Multichannel scaffolds may avoid the complication of lumen collapse observed with the use of single lumen polymer scaffolds.[5,10,15] Multilumen scaffolds have the mechanical and physical attributes to provide an appropriate microenvironment for regeneration.[17,18]

Three broad categories of SCI have been used in animal models: contusion or compression, partial transection, and complete transection. Each offers important contributions to studying repair. Contusion and compression mimic the type of injury that occurs most frequently in patients. However,

Department of Neurology, Mayo Clinic College of Medicine, Rochester, Minnesota.

the occurrence of axonal regeneration and sprouting of the distal segments of surviving axons complicate interpretation of results from studies of contusion and partial transection injury. Complete transection provides a model where factors governing regeneration can be studied in isolation. In addition, the use of scaffolds allows separate manipulation of the three-dimensional structural, cellular, and molecular environment of the regenerating cord.

Neural stem cells (NSCs)[19–21] and Schwann cells (SCs)[15,22,23] have consistently been shown to enhance axonal regeneration within the peripheral and central nervous system (CNS). This study aimed to determine the compatibility of NSCs and SCs with a biodegradable PLGA scaffold and subsequently transplant these cell-loaded scaffolds into the transected spinal cord. Cellular characterization within the scaffold posttransplantation, quantitative assessment of axonal regeneration, and functional recovery using Basso, Beattie, and Bresnahan (BBB) analysis were the major outcome measures. The goal was to determine whether delivery of NSCs and SCs via a scaffold system supported the ability of the cells to promote regeneration, because 40% of patients with SCI have complete loss of function below the level of injury.[1,2] Promoting functional recovery in such patients would require bypassing the destructed spinal cord, and initiating neuron-specific regeneration of axons and path finding to their targets.

Materials and Methods

Fabrication of scaffolds

Scaffolds were fabricated from 85:15 PLGA by an injection molding–solvent evaporation process as previously described.[5] These scaffolds were 2 mm in length, 3 mm in diameter, with seven internal channels, each measuring 660 μm in diameter.

Isolation and culture of NSCs as neurospheres

NSCs were isolated from embryonic day 14.5 rat telencephalon and diencephalon by microdissection, mechanical trituration, and filtering through a 70 μm mesh filter. They were cultured in serum-free media containing DMEM/F12 1:1 (Invitrogen, Grand Island, NY), 1/100 N2 supplement (Invitrogen), 100 IU/mL penicillin–streptomycin (Sigma–Aldrich, St. Louis, MO), 20 ng/mL EGF (PeproTech, Rocky Hill, NJ), and 20 ng/mL bFGF (Sigma–Aldrich). NSCs were cultured as floating neurospheres in low attachment six-well plates, with 4 mL media per well. Neurospheres were passaged, and 2–3 mL of the media per well was replaced every other day. This isolation and culture was adapted from methods previously described.[24–26]

Immunocytochemistry analysis to characterize neurospheres

Neurospheres were characterized *in vitro* by immunocytochemistry using antibodies against nestin (a marker for NSCs, Monoclonal IgG, 1:1000; Chemicon, Temecula, CA), glial fibrillary acidic protein (GFAP) (a marker for astrocytes, polyclonal, 1:150; Promega, Madison, WI), βIII-tubulin (a marker for immature neurons, Monoclonal IgG, 1:250; Chemicon), oligodendrocyte-4 (O4) (a marker for immature oligodendrocytes, Monoclonal IgM, 1:100; Chemicon), and myelin oligodendrocyte-specific protein (MOSP) (a marker for mature oligodendrocytes, Monoclonal IgM, 1:1000; Chemicon). Neurospheres were counterstained with bisbenzimide 33342 (Sigma–Aldrich), which stains cell nuclei. Cyanine 2– and Cyanine 3–conjugated secondary antibodies (Jackson Laboratories, West Grove, PA) were used, and neurospheres were imaged using confocal microscopy (Zeiss Axiovert 100M, Thornwood, NY). For three separate cultures of neurospheres, a random selection of 10 confocal images of neurospheres was taken for each immunostain, using only the bisbenzimide filter to select the section. The proportion of cells positive for each cell marker was determined by dividing the number of cells positive for each marker by the total number of bisbenzimide-stained nuclei.

Isolation, culture, and characterization of primary SCs

SCs were isolated from the sciatic nerve of 2–5-day-old newborn rats, dissociated, and cultured for 24–48 h on laminin (Sigma–Aldrich)–coated tissue culture dishes. Media contained DMEM/F12 (Invitrogen), 10% fetal bovine serum, and 100 IU/mL penicillin–streptomycin (Sigma–Aldrich). SCs were characterized *in vitro* by immunocytochemistry using an antibody against S-100 (polyclonal, 1:10; BioGenex, San Ramon, CA).

Assessment of cell morphology/survival in scaffolds

To assess the distribution of NSCs and SCs within a PLGA scaffold, bisbenzimide 33342 (Sigma–Aldrich)–stained cells were resuspended in undiluted Matrigel (a soluble basement membrane matrix; BD Biosciences, Bedford, MA) and loaded in the seven 660-μm-diameter channels of a 85:15 PLGA scaffold. Scaffolds were ~3 mm in diameter and 2 mm in length. Scaffolds were then cultured in NSC or SC media at 37°C. After fixation with Trump's fixative (4% paraformaldehyde and 1% glutaraldehyde in phosphate buffer pH 7.2), scaffolds were cut in transverse sections using a no. 11 scalpel. Cells in channels were visualized in transverse sections using a Zeiss Axiovert 35 inverted fluorescent microscope.

Preparation of scaffolds for surgeries

Before surgery, scaffolds were sterilized by immersion in 80% ethanol, thoroughly rinsed in distilled water, and then prewet with appropriate cell culture media. Air bubbles were removed by application of a vacuum. Twenty-four hours before implantation, cells (NSCs or SCs) were resuspended in undiluted Matrigel (BD Biosciences) at a density of 10^5 cells/μL and seeded into scaffolds using a pipette with gel-loading pipette tips. Approximately 0.68 μL of cell suspension was required to fill each channel, giving a total of 68,000 cells per channel and 476,000 cells per scaffold. The scaffolds for the control animals were also prewet with cell culture media and were loaded with Matrigel alone without any cells.

Surgery and postoperative care

All procedures involving animals were approved by the Institutional Animal Care and Use Committee at the Mayo Clinic. Adult Sprague-Dawley rats (250–300 g) were anesthetized with 60 mg/kg ketamine (Fort Dodge Animal

Health, Fort Dodge, IA) and 2.5 mg/kg xylazine (Ben Venue Laboratories, Bedford, OH) by intraperitoneal injection. Operations were performed using sterile technique and with the aid of a Zeiss Superlux 40 surgical microscope. A 2 cm midline incision was made along the T7 to T10 spinous processes. The thoracolumbar fascia and paraspinal musculature were incised along the spinous processes and retracted. A T8-9 laminectomy was performed, and the cord was transected using a no. 11 blade, which was confirmed by observation. The site was irrigated with normal saline, and bleeding was controlled using gauze and cotton-tipped applicators. The implant was placed in the transection gap and aligned to assure good contact and no blood clots at the rostral and caudal cord–scaffold interfaces. Because the scaffold was 2 mm in length, all transections resulted in a 2 mm gap between spinal stumps. Surgeries were performed on 42 rats with 17 rats receiving implants containing SCs, 17 rats receiving implants containing NSCs, and 8 rats receiving scaffolds containing no cells (control).

Postoperatively, animals were given buprenorphine 0.05 mg/kg SQ for pain for the first 48 h, Lactated Ringer's solution (LR) as needed, and Enrofloxacin (Bayer, Shawnee Mission, KS) intramuscularly (IM) or Gentamicin (Schering-Plough, Union, NJ) IM for 3–7 days. For the duration of the experiment, bladder voiding and observation of the animals were performed twice daily. Enrofloxacin or Gentamicin and Lactated Ringer's solution were used to treat urinary tract infections, and topical antibiotics were used to treat decubital ulcers.

Functional analysis

Functional recovery of experimental and control animals was assessed by performing open field testing using the BBB locomotor rating scale 2 and 4 weeks after surgery.[27] Each rat was observed in an open plastic box for 5 min, and three independent, blinded observers recorded hind limb joint movements, weight support, toe clearance, tail position, and coordination of gait and paw position. Observations were used to give each rat a rating on the 21-point BBB locomotor rating scale.

Histological and immunohistochemical analysis

One month after surgery, animals were euthanized with pentobarbital (Fort Dodge Animal Health) IM and fixed by transcardial perfusion with 4% paraformaldehyde. The spinal column was removed en bloc and postfixed in 4% paraformaldehyde for 48 h. The spinal cord was then removed and postfixed in 4% paraformaldehyde for an additional 24–48 h. A 1 cm region of the spinal cord containing the scaffold was embedded in paraffin and 8-μm-thick serial transverse sections cut with a Reichert Jung tabletop microtome (Leica, Heidelberg, Germany). Longitudinal sections were cut for one animal from each group.

Characterization of cells within the scaffolds used the same immunohistochemical staining as described for the neurospheres. Antibodies against adenomatous polyposis coli (APC; monoclonal IgG, 1:20; Calbiochem, San Diego, CA), galactocerebroside (Gal-C; polyclonal, 1:1000; Sigma–Aldrich), and neurofilament (monoclonal IgG, 1:100; Dako, Carpinteria, CA) were also included in the analysis. Cy2- or Cy3-conjugated secondary antibodies (Jackson Laboratories) or 3-amino-9-ethylcarbarzole (AEC) (Dako) were used for primary antibody detection. For each animal, sections from one quarter, one half, and three quarters of the way through the scaffold were stained with each antibody.

Axonal profile counting and data analysis

Neurofilament staining was used to identify axons within the channels of the scaffold. Serial transverse sections one quarter, one half, and three quarters of the way through the scaffold were stained with mouse monoclonal anti-neurofilament antibody (as above). One section was randomly selected at each level for data analysis. Individual channels within scaffolds were identified and the area outlined. For each animal, the total axon number within the scaffold channels was counted by a blinded observer. Each level of the animal (i.e., one quarter, one half, or three quarters) was analyzed as a separate data point. Because a given level, for example, one quarter, was representative of axons growing from the rostral cord and another level, for example, three quarters, represented axons growing from the caudal cord, these observations were treated as independent. Kruskal–Wallis test (nonparametric ANOVA) was used to determine if there was a significant difference in median axonal counts between the three groups.

Results

Results of surgery and animal survival

Surgeries were performed on 42 rats with 17 rats receiving implants containing SCs, 17 rats receiving implants containing NSCs, and 8 rats receiving scaffolds containing no cells (control). Of these animals, four rats were excluded due to severe self-mutilation requiring early euthanasia. Data were analyzed from 14 rats in the NSC group, 16 rats in the SC group, and 8 rats in the control group. There was some evidence of increased pain behavior in the NSC-treated group. There was severe self-mutilation in three rats within this group compared to only one rat in the SC group.

Characterization of NSCs and SCs

NSCs, grown *in vitro* as neurospheres (Fig. 1A), were characterized using immunocytochemical staining for nestin (Fig. 1B), βIII tubulin (Fig. 1C), GFAP (Fig. 1D), O4 (Fig. 1E), and MOSP (Fig. 1F). Cellular morphology was consistent with the specificity of the stains. About $81.5 \pm 1.96\%$ of cells were nestin positive; $0.44 \pm 0.21\%$ of cells were βIII-tubulin positive; $3.2 \pm 0.82\%$ of cells were GFAP positive; $11.8 \pm 1.43\%$ of cells were O4 positive; and $2.8 \pm 1.04\%$ of cells were MOSP positive. Isolated SCs exhibited typical bipolar morphology (Fig. 1G) and were characterized by immunocytochemical staining for S-100 (Fig. 1H). About $91.95 \pm 2.2\%$ of cells expressed the marker.

Morphology and survival of NSCs and SCs when cultured within a PLGA scaffold

NSCs and SCs stained with bisbenzimide 33342 were loaded into the seven longitudinal channels of each PLGA scaffold (Fig. 2A). Over a period of 3 days in culture, the NSCs and SCs showed an even distribution within the channels and continued to proliferate within the scaffold as

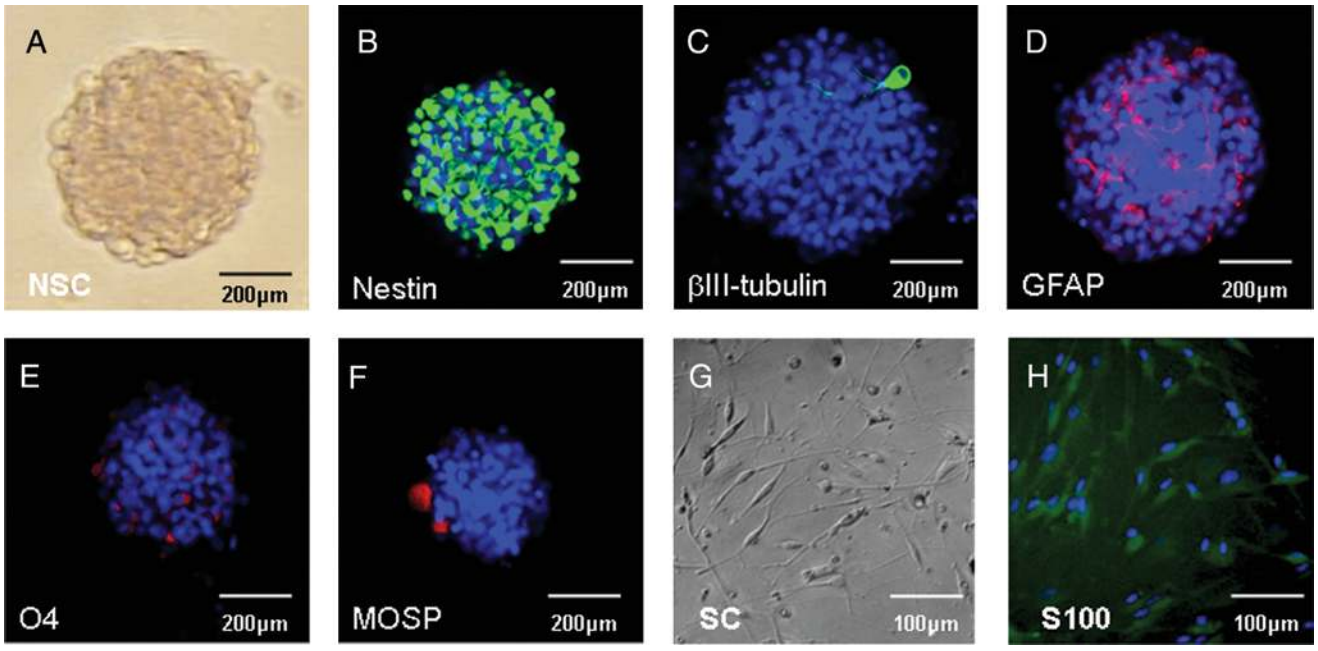

FIG. 1. Characterization of NSCs and SCs *in vitro*. Phase contrast image of a neurosphere in culture (**A**). Confocal microscopy images of neurospheres stained with Nestin (**B**), βIII-tubulin (**C**), GFAP (**D**), O4 (**E**), and MOSP (**F**). Bisbenzimide (blue) was used to counterstain the nuclei of all cells in (**B–F**). Phase contrast image of SCs in culture (**G**). Fluorescent microscopy image of SCs stained with S100 (**H**). Magnification: 100 × (**A–F**); 200 × (**G, H**). Color images available online at www.liebertonline.com/ten.

shown at 2 h (Fig. 2B, D) and at 65 h (Fig. 2C, E), respectively. When left to incubate within the scaffold, NSCs were shown to be able to differentiate as demonstrated by βIII tubulin–positive staining (Fig. 2F).

Characterization of cells within the scaffolds after delivery to the transected cord

Animals were sacrificed 1 month posttransplantation of the scaffolds, and their spinal cords were harvested for histology. Immunocytochemical analysis revealed the presence of nestin (Fig. 3A), neurofilament (Fig. 3B), βIII tubulin (Fig. 3C), Gal C (Fig. 3C), and APC (Fig. 3D) expressing cells within the NSC-loaded scaffolds.

Animals that received SC-loaded scaffolds showed expression of S-100 within the channels (Fig. 3E), as well as other neural markers such as APC (Fig. 3F) and neurofilament (Fig. 3G–I). The location at which these images were taken is represented in the schematic in Figure 3J.

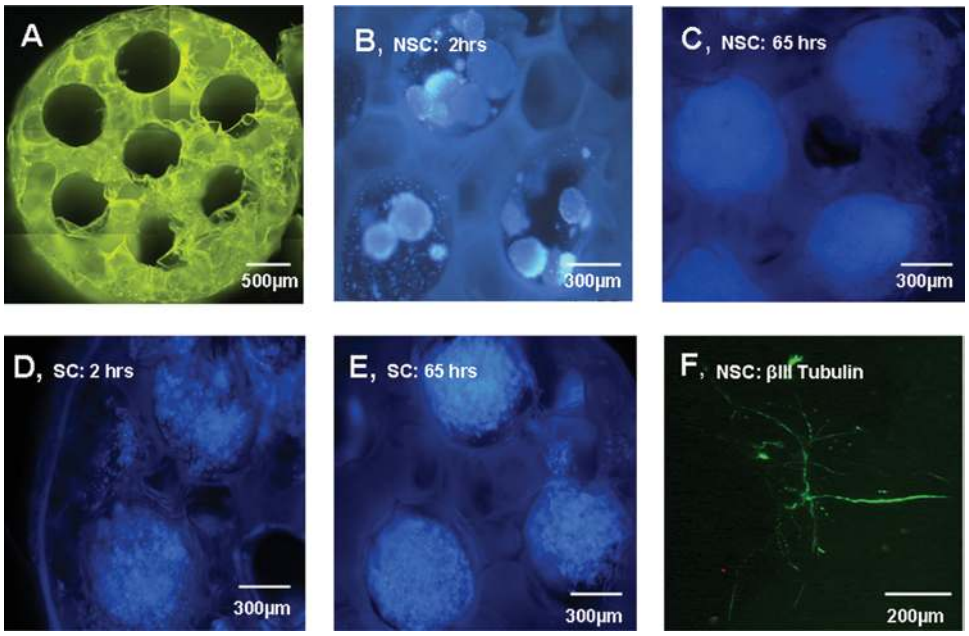

FIG. 2. NSC and SC survival/morphology when loaded into PLGA scaffolds *in vitro*. The 85:15 PLGA scaffolds were 2 mm in length, 3 mm in diameter, and contained 660-μm-diameter longitudinal channels (**A**). Autofluorescence of the scaffolds occurred. Neurospheres or SCs, stained with bisbenzimide 33342 (blue), were evenly distributed in the channels after 2 h in culture (**B, D**), and proliferated to fill the channels after 65 h in culture (**C, E**), respectively. NSCs retained their ability to differentiate when cultured in the scaffold (**F**) (taken 24 h postseeding). All images were taken transversely at the end of the scaffold channels using a confocal microscope. Magnification: 25× (**A**); 50 × (**B–E**); 100 × (**F**). Color images available online at www.liebertonline.com/ten.

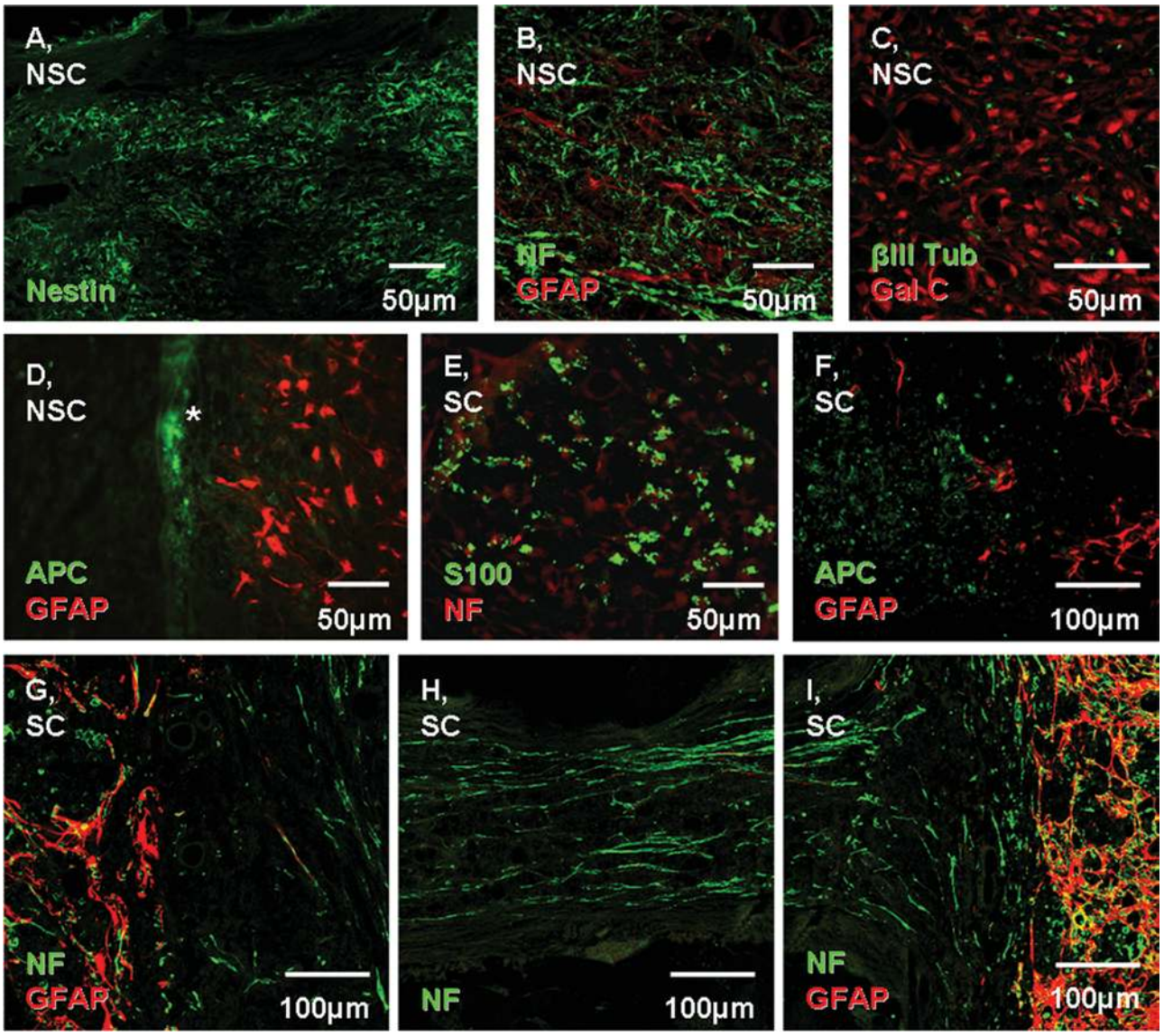

FIG. 3. Characterization of cells within the scaffolds 1 month after transplantation into the transected cord. Confocal (**A–C, E, G–I**) and fluorescent (**D, F**) microscopy images of nestin (**A**), neurofilament (NF) (**B, E, G–I**), GFAP (**B, D, F, G–I**), βIII tubulin (**C**), Gal C (**C**), APC (**D, F**), stained cells in NSC-loaded (**A–D**), and SC-loaded (**E–I**) channels. Transverse sections: (**C, E**). Longitudinal sections: (**A, B, D, F–I**). (**J**) Schematic representation of the location at which images (**A–I**) were taken in the scaffold. In image (**D**) asterisk (*) denotes the border between the spinal cord and scaffold. Magnification: 200 × (**F–I**); 400 × (**A, B, D, E**); 630 × (**C**). Color images available online at www.liebertonline.com/ten.

Quantitative comparison of axonal regeneration

Neurofilament staining was used to quantify axonal regeneration within the NSC-treated (Fig. 4B), SC-treated (Fig. 4C), or control-treated (Fig. 4D) groups. For each animal, the total number of axons within the scaffold was counted in transverse sections selected from one quarter, one half, and three quarters of the way through the scaffold (Fig. 4A).

Axons were found not only in distinct channels, but also in pores within the biodegradable scaffold. As seen in Figure 2A, the scaffold is not solid, but spongy and contains pores within the polymer material. Thus, it was often not possible to identify seven distinct channels. For this reason and the fact that channels within an individual animal are not independent observations, the total number of axons per transverse section was analyzed rather than the number of axons per channel.

Figure 4E shows the distribution of axonal counts between each group. Comparison of the number of axons per channel at the individual levels (one quarter, one half, and three quarters) did not show significant differences between groups at each level or between levels. However, if data from all levels were pooled, there were significantly more axons in the cell-loaded scaffolds compared with controls. An alternative method of analysis would be to average the data from all channels at each level of an animal to generate single independent observations. One-way ANOVA revealed that the medians of the three different groups varied significantly ($p < 0.05$). The Kruskal–Wallis test produced a p-value of 0.016. Both the NSC- and SC-treated groups had a greater number of axonal profiles within the channels when compared to the control group that received no cells. The SC-treated group also showed a trend toward greater axonal counts when compared to the NSC-treated group.

Functional analysis

Recovery of locomotor function was assessed using the BBB rating scale. While there were significant differences in the axonal counts in the NSC and SC versus the control group, this did not have any impact on the functional recovery seen. No significant difference in BBB scores was evidenced between the groups tested. The BBB scores for the 2 week time-point were 2.51 ± 0.9, 1.22 ± 0.49, and

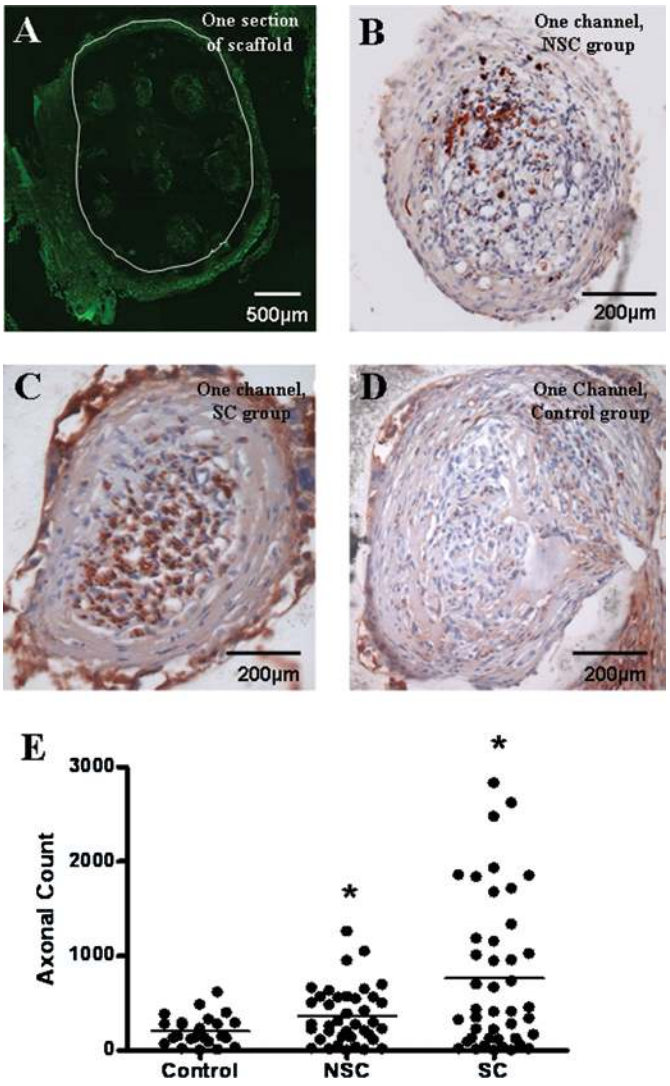

FIG. 4. Neurofilament staining of axons in transverse sections through the scaffold after 1 month *in vivo*. Fluorescent microscopy image of one transverse section of a scaffold (loaded with NSCs) stained with an antibody against neurofilament with the region in which axons were counted encircled by a white line (**A**). Transverse sections of one channel from the NSC group (**B**), one from the SC group (**C**), and one from the control group (**D**) stained for neurofilament using an AEC chromogen. Magnification: 25× (**A**); 100× (**B–D**). Dot plots of axonal counts per cord in the NSC-, SC-, and control-treated groups (**E**). Data points represent individual animals. 95% Confidence interval was used for each group. *Medians vary significantly ($p < 0.05$) ($p = 0.0162$ using the Kruskal–Wallis test) when compared to the control group. Color images available online at www.liebertonline.com/ten.

0.78 ± 0.30 for the control, NSC, and SC groups, respectively. The 4 week time-point scores were 0.96 ± 0.04, 1.92 ± 0.43, and 1.14 ± 0.45 for the control, NSC, and SC groups, respectively.

Discussion

This study demonstrated that multichannel biodegradable polymer scaffolds effectively serve as platforms for quantitatively assessing axonal regeneration after SCI. This was due, in part, to the nature of the transection model. Both NSCs and SCs seeded in a multichannel biodegradable polymer scaffold supported axonal regeneration after spinal cord transection in rats, with a trend toward greater axonal regeneration in the SC-treated group.

Immunohistochemical analysis of the scaffolds 1 month posttransplantation revealed extensive nestin and neurofilament staining throughout the scaffold in the NSC-treated group. APC was more prominently localized at the border between the spinal cord and the scaffold (denoted by the * in Fig. 3D), while GFAP-positive cells were mainly located in the spinal cord without extending into the scaffold. Nestin was the most frequently positive marker in the NSC-treated group *in vivo*. Nestin is primarily expressed in the developing CNS. It is, however, also expressed in adult cells, including NSCs, and is upregulated after CNS injury. Nestin expression has also been shown in radial glial cells, ependymal cells, and in reactive astrocytes after CNS injury in rats.[28–30]

In previous studies of NSC transplantation in adult rat models of SCI, NSCs have primarily differentiated into astrocytes or remained undifferentiated.[20,31,32] This is in contrast to our findings that show no differentiation into GFAP-expressing cells within the channels. This observation is very interesting and will require further investigation to determine whether the environment in the channel diverts NSC differentiation away from the astrocyte lineage or that it prevents astrocyte precursors from entering the channel. We speculate that within the channel the regenerating axons are in a localized microenvironment that has different properties from the microenvironment of the adjacent spinal cord. The adjacent spinal cord contains all of the injury response elements that facilitate astrocyte differentiation and scar formation. The environment within the channel is restricted to regenerating tissue. This may have implications for the prevention of glial scarring.

Immunohistochemical analysis of the SC-loaded scaffolds revealed S-100 staining within the channels. Extensive neurofilament staining throughout the SC-loaded scaffold suggests that axons traversing the channels were from neurons on either side of the scaffold. The SCs appear to attract adjacent neurons to project regenerating axons from the injured cord into the scaffold and to provide a structural support upon which axonal growth can take place.

The quantitative assessment of regeneration by axonal counting was feasible due to the nature of the complete transection model. The multichannel scaffold provided clearly defined regions in which to count axons, and because all axons were transected at the time of injury, we could be sure that the observed regeneration was not as a result of sprouting from residual nontransected axons. There were a greater number of axons in the NSC- and SC-treated groups when compared to the control group, with a trend toward greater axonal counts in the SC-treated group. Lack of neuronal cell body staining within the channels strengthens the argument that neurofilament-stained axons were from endogenous cells regenerating into the rostral and caudal injured cord. The absolute numbers of axons in each of the cell-treated groups were relatively small (<3000 axons in transverse section) compared to the total number of axons in the normal spinal cord. We have previously counted a total of $260{,}000 \pm 20{,}000$ axons in transverse sections of the uninjured rat thoracic spinal cord (unpublished observations). Although achieving growth of axons into the channels of the scaffold is an accomplishment, for functional recovery to be achieved, axons need to traverse the scaffold, exit the opposite scaffold–cord interface, reach appropriate targets, and form functional synapses. Bregman *et al.* estimated that 5–10% of corticospinal axons are needed to promote functional recovery after SCI.[33] This estimate is consistent with the lack of functional improvement in this study where about 1% of axons regenerated. The use of a longer time-point could potentially demonstrate significant behavioral improvement after delivery of one or both of the cell types.

Previous studies demonstrate increased allodynia after transplantation of NSCs in a contusion model of SCI in rats.[34] This is consistent with our findings where there was a trend toward increased pain behavior (i.e., autophagia) associated with the NSC-treated group. Several of the animals were lost from the study because of this severe self-mutilation, which was more frequent in the NSC-treated group.

This work represents an evolving model for treatment of severe SCI. The results point to several avenues of future research. Identifying the best cell type for promoting axonal regeneration is of great importance in optimizing the model. This study demonstrated the compatibility of NSCs and SCs within polymer scaffolds and their potential for promoting regeneration within a transection injury. Future studies will focus on altering this environment by selectively expressing neuronal growth or axonal guidance factors to increase the level of regeneration of specific neurons. Potential synergistic interactions between cells and growth factors within one channel and the potential to regionally direct axonal growth by aligning specific cell types with spinal cord tracts will also be studied.[3]

Conclusion

In conclusion, this study demonstrates that biodegradable scaffolds with aligned columns seeded with NSCs or SCs facilitate regeneration across the transected spinal cord. Further, these multichannel biodegradable polymer scaffolds effectively serve as platforms for quantitative analysis of axonal regeneration.

Acknowledgments

Grant support was provided by NIH (EB002390) and the Wilson, Morton, and Mayo Foundations. Dr. Jason Eriksen and Hyun-hee Kim from Mayo Clinic in Jacksonville, FL, were helpful in developing a method for culturing and immunostaining neurospheres. Jesse Voss provided assistance with axonal counting. The excellent secretarial support of Ms. Jane Meyer is greatly appreciated.

Disclosure Statement

No competing financial interests exist among any of the authors.

References

1. Quencer, R.M., and Bunge, R.P. The injured spinal cord: imaging, histopathologic clinical correlates, and basic science approaches to enhancing neural function after spinal cord injury. Spine **21,** 2064, 1996.
2. Bodley, R. Imaging in chronic spinal cord injury—indications and benefits. Eur J Radiol **42,** 135, 2002.
3. Friedman, J.A., Windebank, A.J., Moore, M.J., Spinner, R.J., Currier, B.L., and Yaszemski, M.J. Biodegradable polymer grafts for surgical repair of the injured spinal cord. Neurosurgery **51,** 742, 2002.
4. Novikova, L.N., Novikov, L.N., and Kellerth, J.O. Biopolymers and biodegradable smart implants for tissue regeneration after spinal cord injury. Curr Opin Neurol **16,** 711, 2003.
5. Moore, M.J., Friedman, J.A., Lewellyn, E.B., Mantila, S.M., Krych, A.J., Ameenuddin, S., Knight, A.M., Lu, L., Currier, B.L., Spinner, R.J., Marsh, R.W., Windebank, A.J., and Yaszemski, M.J. Multiple-channel scaffolds to promote spinal cord axon regeneration. Biomaterials **27,** 419, 2006.
6. Athanasiou, K.A., Niederauer, G.G., and Agrawal, C.M. Sterilization, toxicity, biocompatibility and clinical applications of polylactic acid/polyglycolic acid copolymers. Biomaterials **17,** 93, 1996.
7. Dalbasti, T., Oktar, N., Cagli, S., and Ozdamar, N. Local interstitial chemotherapy with sustained release bucladesine in *de novo* glioblastoma multiforme: a preliminary study. J Neurooncol **56,** 167, 2002.
8. Fournier, E., Passirani, C., Montero-Menei, C.N., and Benoit, J.P. Biocompatibility of implantable synthetic polymeric drug carriers: focus on brain biocompatibility. Biomaterials **24,** 3311, 2003.
9. Rokkanen, P.U., Bostman, O., Hirvensalo, E., Makela, E.A., Partio, E.K., Patiala, H., Vainionpaa, S.I., Vihtonen, K., and Tormala, P. Bioabsorbable fixation in orthopaedic surgery and traumatology. Biomaterials **21,** 2607, 2000.
10. Weber, R.A., Breidenbach, W.C., Brown, R.E., Jabaley, M.E., and Mass, D.P. A randomized prospective study of polyglycolic acid conduits for digital nerve reconstruction in humans. Plast Reconstr Surg **106,** 1036, 2000.
11. Reid, R.L., Cutright, D.E., and Garrison, J.S. Biodegradable cuff an adjunct to peripheral nerve repair: a study in dogs. Hand **10,** 259, 1978.
12. Meek, M.F., den Dunnen, W.F., Robinson, P.H., Pennings, A.J., and Schakenraad, J.M. Evaluation of functional nerve recovery after reconstruction with a new biodegradable poly (DL-lactide-epsilon-caprolactone) nerve guide. Int J Artif Organs **20,** 463, 1997.
13. Meek, M.F., Robinson, P.H., Stokroos, I., Blaauw, E.H., Kors, G., and den Dunnen, W.F. Electronmicroscopical evaluation of short-term nerve regeneration through a thin-walled biodegradable poly(DLLA-epsilon-CL) nerve guide filled with modified denatured muscle tissue. Biomaterials **22,** 1177, 2001.
14. Gautier, S.E., Oudega, M., Fragoso, M., Chapon, P., Plant, G.W., Bunge, M.B., and Parel, J.M. Poly(alpha-hydroxyacids) for application in the spinal cord: resorbability and biocompatibility with adult rat Schwann cells and spinal cord. J Biomed Mater Res **42,** 642, 1998.
15. Oudega, M., Gautier, S.E., Chapon, P., Fragoso, M., Bates, M.L., Parel, J.M., and Bunge, M.B. Axonal regeneration into Schwann cell grafts within resorbable poly(alpha-hydroxyacid) guidance channels in the adult rat spinal cord. Biomaterials **22,** 1125, 2001.
16. Pinzon, A., Calancie, B., Oudega, M., and Noga, B.R. Conduction of impulses by axons regenerated in a Schwann cell graft in the transected adult rat thoracic spinal cord. J Neurosci Res **64,** 533, 2001.
17. Moore, M.J., Jabbari, E., Ritman, E.L., Lu, L., Currier, B.L., Windebank, A.J., and Yaszemski, M.J. Quantitative analysis of interconnectivity of porous biodegradable scaffolds with micro-computed tomography. J Biomed Mater Res **71,** 258, 2004.
18. Ruiter, G.D., Onyeneho, I., Liang, E., Moore, M., Knight, A.M., Malessy, M., Spinner, R., Lu, L., Currier, B., Yaszemski, M., and Windebank, A. Methods for *in vitro* characterization of multichannel nerve tubes. J Biomed Mater Res A, **84,** 643, 2007.
19. Cao, Q., Benton, R.L., and Whittemore, S.R. Stem cell repair of central nervous system injury. J Neurosci Res **68,** 501, 2002.
20. Wu, S., Suzuki, Y., Kitada, M., Kitaura, M., Kataoka, K., Takahashi, J., Ide, C., and Nishimura, Y. Migration, integration, and differentiation of hippocampus-derived neurosphere cells after transplantation into injured rat spinal cord. Neurosci Lett **312,** 173, 2001.
21. Lu, P., Jones, L.L., Snyder, E.Y., and Tuszynski, M.H. Neural stem cells constitutively secrete neurotrophic factors and promote extensive host axonal growth after spinal cord injury. Exp Neurol **181,** 115, 2003.
22. Xu, X.M., Guenard, V., Kleitman, N., and Bunge, M.B. Axonal regeneration into Schwann cell-seeded guidance channels grafted into transected adult rat spinal cord. J Comp Neurol **351,** 145, 1995.
23. Takami, T., Oudega, M., Bates, M.L., Wood, P.M., Kleitman, N., and Bunge, M.B. Schwann cell but not olfactory ensheathing glia transplants improve hindlimb locomotor performance in the moderately contused adult rat thoracic spinal cord. J Neurosci **22,** 6670, 2002.
24. Reynolds, B.A., and Weiss, S. Generation of neurons and astrocytes from isolated cells of the adult mammalian central nervous system. Science **255,** 1707, 1992.
25. Reynolds, B.A., and Weiss, S. Clonal and population analyses demonstrate that an EGF-responsive mammalian embryonic CNS precursor is a stem cell. Dev Biol **175,** 1, 1996.
26. Lobo, M.V., Alonso, F.J., Redondo, C., Lopez-Toledano, M.A., Caso, E., Herranz, A.S., Paino, C.L., Reimers, D., and Bazan, E. Cellular characterization of epidermal growth factor-expanded free-floating neurospheres. J Histochem Cytochem **51,** 89, 2003.
27. Basso, D.M., Beattie, M.S., and Bresnahan, J.C. A sensitive and reliable locomotor rating scale for open field testing in rats. J Neurotrauma **12,** 1, 1995.
28. Schwab, J.M., Beschorner, R., Nguyen, T.D., Meyermann, R., and Schluesener, H.J. Differential cellular accumulation of connective tissue growth factor defines a subset of reactive astrocytes, invading fibroblasts, and endothelial cells following central nervous system injury in rats and humans. J Neurotrauma **18,** 377, 2001.
29. Shibuya, S., Miyamoto, O., Auer, R.N., Itano, T., Mori, S., and Norimatsu, H. Embryonic intermediate filament, nestin, expression following traumatic spinal cord injury in adult rats. Neuroscience **114,** 905, 2002.
30. Shibuya, S., Miyamoto, O., Itano, T., Mori, S., and Norimatsu, H. Temporal progressive antigen expression in radial glia after contusive spinal cord injury in adult rats. Glia **42,** 172, 2003.

31. Ogawa, Y., Sawamoto, K., Miyata, T., Miyao, S., Watanabe, M., Nakamura, M., Bregman, B.S., Koike, M., Uchiyama, Y., Toyama, Y., and Okano, H. Transplantation of *in vitro*-expanded fetal neural progenitor cells results in neurogenesis and functional recovery after spinal cord contusion injury in adult rats. J Neurosci Res **69,** 925, 2002.
32. Cao, Q.L., Zhang, Y.P., Howard, R.M., Walters, W.M., Tsoulfas, P., and Whittemore, S.R. Pluripotent stem cells engrafted into the normal or lesioned adult rat spinal cord are restricted to a glial lineage. Exp Neurol **167,** 48, 2001.
33. Bregman, B.S., Kunkel-Bagden, E., Schnell, L., Dai, H.N., Gao, D., and Schwab, M.E. Recovery from spinal cord injury mediated by antibodies to neurite growth inhibitors. Nature **378,** 498, 1995.
34. Hofstetter, C.P., Holmstrom, N.A., Lilja, J.A., Schweinhardt, P., Hao, J., Spenger, C., Wiesenfeld-Hallin, Z., Kurpad, S.N., Frisen, J., and Olson, L. Allodynia limits the usefulness of intraspinal neural stem cell grafts; directed differentiation improves outcome. Nat Neurosci **8,** 346, 2005.

Address correspondence to:
Anthony J. Windebank, M.D.
Mayo Clinic College of Medicine
15 Guggenheim Building
200 First St. SW
Rochester, MN 55905

E-mail: windebank.anthony@mayo.edu

Received: June 30, 2008
Accepted: November 7, 2008
Online Publication Date: January 30, 2009